

# Study of the Properties of Co-Substituted Ba<sub>2</sub>Mg<sub>2</sub>Fe<sub>12</sub>O<sub>22</sub> Hexaferrites

Tatyana Koutzarova <sup>1,\*</sup>, Borislava Georgieva <sup>1</sup>, Svetoslav Kolev <sup>1</sup>, Kiril Krezhov <sup>1</sup>, Daniela Kovacheva <sup>2</sup>, Chavdar Ghelev <sup>1</sup>, Benedicte Vertruyen <sup>3</sup>, Frederic Boschini <sup>3</sup>, Abdelfattah Mahmoud <sup>3</sup>, Lan Maria Tran <sup>4</sup>, and Andrzej Zaleski <sup>4</sup>

<sup>1</sup> Institute of Electronics, Bulgarian Academy of Sciences, 72 Tsarigradsko Chaussee, 1784 Sofia, Bulgaria; tatyana\_koutzarova@yahoo.com, b.georgiewa@abv.bg, svet\_kolev@yahoo.com, kiril.krezhov@gmail.com, chavdarghelev@yahoo.com

<sup>2</sup> Institute of General and Inorganic Chemistry, Bulgarian Academy of Sciences, Acad. Georgi Bonchev Str., bld. 11, 1113 Sofia, Bulgaria; dkovacheva@gmail.com

<sup>3</sup> Greenmat, Chemistry Department, University of Liege, 11 allée du 6 août, 4000 Liège, Belgium; b.vertruyen@uliege.be, frederic.boschini@uliege.be, abdefattah.mahmoud@uliege.be

<sup>4</sup> Institute of Low Temperature and Structure Research, Polish Academy of Sciences, Ul. Okólna 2, 50-422 Wrocław, Poland; l.m.tran@intibs.pl, a.zaleski@int.pan.wroc.pl

\* Correspondence: tatyana\_koutzarova@yahoo.com, tanya@ie.bas.bg ; Tel.: +359-2-979-5871

Received: 24 April 2018; Accepted: 26 April 2018; Published: 17 May 2018

**Abstract:** We present results from a study on the influence of the substitution of Mg<sup>2+</sup> cations in the Y-type Ba<sub>2</sub>Mg<sub>2</sub>Fe<sub>12</sub>O<sub>22</sub> hexaferrite with magnetic cations, such as Co<sup>2+</sup>, on its structural and magnetic properties. The Ba<sub>2</sub>Mg<sub>0.4</sub>Co<sub>1.6</sub>Fe<sub>12</sub>O<sub>22</sub> powder was synthesized by sonochemical co-precipitation method. The XRD pattern of the powders showed the characteristic peaks corresponding to the Y-type hexaferrite structure as a main phase and some CoFe<sub>2</sub>O<sub>4</sub> impurity (< 2%) as a second phase. This result was also confirmed by Mössbauer spectroscopy measurements. The magnetization values at 50 kOe were 30 emu/g at 4.2 K and 26.6 emu/g at 300 K, respectively. The ZFC and FC magnetization curves were measured at magnetic fields of 50 Oe, 100 Oe and 500 Oe, which revealed a magnetic phase transition around 200 K from ferrimagnetic-to-helical spin order. This is considered as a precondition for the material to exhibit multiferroic properties.

**Keywords:** sonochemical co-precipitation; Y-type hexaferrite; Mossbauer spectroscopy; magnetic properties; magnetic-phase transition

---

## 1. Introduction

Multiferroic materials form a special class of magnetic materials. In them, long-range magnetic and ferroelectric orders coexist, a property that has provoked keen researchers' interest from both basic and practical points of view [1, 2]. The magneto-electric multiferroics are materials that combine coupled electric and magnetic dipoles [3]. Research in the past decade has demonstrated that magneto-electric effect can be induced by complex internal arrangements of magnetic moments in some hexaferrites. One of the first magnetoelectric hexaferrites discovered was Ba<sub>2</sub>Mg<sub>2</sub>Fe<sub>12</sub>O<sub>22</sub>. It has a relatively high spiral-magnetic transition temperature (~200 K), shows multiferroic properties at zero magnetic field and the direction of the electric polarization can be governed by relatively low magnetic fields (<0.02 T) [4].

Ba<sub>2</sub>Mg<sub>2</sub>Fe<sub>12</sub>O<sub>22</sub> is representative of the family of Y-type hexaferrites Ba<sub>2</sub>Me<sub>2</sub>Fe<sub>12</sub>O<sub>22</sub>, where Me is a divalent cation which adopts a structural type described by the space group R-3m. All the cations (Me<sup>+2</sup> and Fe<sup>+3</sup>) are distributed over six distinct crystallographic sites: two tetrahedral sites (6c<sub>IV</sub> and 6c\*<sub>IV</sub>) and four octahedral sites (3a<sub>VI</sub>, 3b<sub>VI</sub>, 6c<sub>VI</sub>, and 18h<sub>VI</sub>). The type of these divalent cations, as well as the site they occupy within the unit cell can result in significant modifications of the structural and

magnetic properties. The unit cell contains three formula units and is built from sequential stacking of the S and the T-blocks in a sequence of (TST'ST''S'') where the primes indicate a rotation about the *c*-axis by 120 degrees; the easy magnetization axis lies in a plane normal to the *c* axis direction [5]. The magnetic structure can be represented by two magnetic sublattice *L* and *S* blocks stacked alternately along [001], which bear, respectively, opposite large and small magnetization *M*. For Ba<sub>2</sub>Mg<sub>2</sub>Fe<sub>12</sub>O<sub>22</sub> at temperatures exceeding room temperature (below 553 K) a ferrimagnetic spin arrangement sets in, and below 195 K a proper screw spin structure was identified [6, 7]. The turn angle of the helix is about 70° [8].

Magnetic measurements of Ba<sub>2</sub>Mg<sub>2</sub>Fe<sub>12</sub>O<sub>22</sub> single crystals have demonstrated a transition to a longitudinal-conical spin state below about 50 K [9].

In our previous studies [10, 11] we showed that in a Ba<sub>2</sub>Mg<sub>2</sub>Fe<sub>12</sub>O<sub>22</sub> powder material synthesized by sonochemical co-precipitation the magnetic phase transition from ferromagnetic-to-spiral spin order occurs at 196 K at a magnetic field of 100 Oe.

We present here results from a study on the influence of cobalt substitution for magnesium in the Y-type Ba<sub>2</sub>Mg<sub>2</sub>Fe<sub>12</sub>O<sub>22</sub> hexaferrite on its structural and magnetic properties. We pay special attention to the changes in the magnetic-phase transition temperature due to the partial major substitution of the nonmagnetic Mg<sup>2+</sup>cations with magnetic Co<sup>2+</sup> cations and to the influence of external magnetic field..

## 2. Materials and Methods

The Ba<sub>2</sub>Mg<sub>0.4</sub>Co<sub>1.6</sub>Fe<sub>12</sub>O<sub>22</sub> powder material was synthesized by sonochemical co-precipitation. Stoichiometric amounts of corresponding metal nitrates, such as Co(NO<sub>3</sub>)<sub>2</sub>·6H<sub>2</sub>O, Mg(NO<sub>3</sub>)<sub>2</sub>·6H<sub>2</sub>O and Fe(NO<sub>3</sub>)<sub>3</sub>·9H<sub>2</sub>O, and 10 wt % of over-stoichiometric Ba(NO<sub>3</sub>)<sub>2</sub>, were dissolved completely in deionized water and, after homogenization, the co-precipitation process was initiated by adding NaOH at pH = 11.5. High-power ultrasound stirring was applied to assist this process, which, as is known, enhances the reaction rate, the mass transport and the thermal effects. The ultrasound with amplitude 40 % was applied for 15 min by a Sonics ultrasonic processor (750 W). The precipitate was separated in a centrifuge, dried and milled. The as-obtained precursor was calcined at 700 °C under air and then subjected to thermal treatment at 1170 °C for 7 hours under air to obtain the final material - Ba<sub>2</sub>Mg<sub>0.4</sub>Co<sub>1.6</sub>Fe<sub>12</sub>O<sub>22</sub>.

The as prepared Ba<sub>2</sub>Mg<sub>0.4</sub>Co<sub>1.6</sub>Fe<sub>12</sub>O<sub>22</sub> powders were characterized by X-ray diffraction (XRD) for phase identification, Mössbauer spectroscopy (MS) and magnetization measurements.

The XRD patterns were taken at ambient temperature on a Bruker D8 diffractometer (40 kV, 30 mA) controlled by a DIFFRACTPLUS software, in Bragg-Brentano reflection geometry with Cu-K $\alpha$  radiation ( $\lambda = 1.5418 \text{ \AA}$ ), Iron-57 Mössbauer spectroscopy was used to probe the oxidation state of iron ions and investigate their coordinations. The <sup>57</sup>Fe transmission Mössbauer spectroscopy data were recorded by a constant-acceleration spectrometer with a <sup>57</sup>Co(Rh) source at room temperature. The Mössbauer spectrum absorber was prepared using 40 mg/cm<sup>2</sup> of material mixed with boron nitride. The spectrometer was calibrated at room temperature with the magnetically split sextet spectrum of a high-purity  $\alpha$ -Fe foil as the reference absorber. The measurements were carried out in the ( $\pm 12$  mm/s) velocity range. The spectral parameters, namely, the isomer shift ( $\delta$ ), the quadrupole splitting ( $\Delta$ ), the linewidth ( $\Gamma$ ), the magnetic field ( $B_{\text{hf}}$ ) and the relative resonance areas of the different spectral components were determined by fitting the experimental data. The fits' validity was judged on the basis of minimizing the number of parameters and  $\chi^2$  values.

The magnetic properties were measured by using a SQUID Quantum Design magnetometer. The hysteresis measurements were conducted at 4.2 K and at room temperature. The zero-field-cooled (ZFC) and field-cooled (FC) magnetization vs. temperature (4.2 – 300 K) measurements were performed at magnetic fields of 50 Oe, 100 Oe and 500 Oe. In the ZFC protocol, the sample under study was cooled from room temperature to 4.2 K without any magnetic field, and the magnetization was measured during heating from 4.2 – 300 K at a heating rate of 3 K/min under the applied magnetic field. The FC curve was recorded on the same sample upon cooling from 300 K to 4.2 K under the same magnetic field.

### 3. Results and Discussion

The XRD pattern of the  $\text{Ba}_2\text{Mg}_{0.4}\text{Co}_{1.6}\text{Fe}_{12}\text{O}_{22}$  powder material is shown in Figure 1. The XRD result showed the characteristic peaks corresponding to the Y-type hexaferrite structure as a main phase and some  $\text{CoFe}_2\text{O}_4$  impurity (< 2 %) as a negligible second phase. This small amount of the second phase did not affect strongly the sample's magnetic properties, as it can be seen in Figure 3.

The lattice cell parameters and cell volume of the samples were calculated after indexing of the measured diffraction peaks from the following equation [12]:

$$d_{hkl} = \frac{1}{\sqrt{4\frac{(h^2+h^2+k^2)}{3a^2} + \frac{l^2}{c^2}}} \quad (1)$$

where  $d_{hkl}$  is the d-spacing of the lines in the XRD pattern, and  $h$ ,  $k$  and  $l$  are the corresponding Miller indices. The lattice constant  $a$  and  $c$  are 5.88(5) Å and 43.58(4) Å, respectively. These results for unit cell parameters are in good agreement with the values published earlier for the  $\text{Ba}_2\text{Mg}_2\text{Fe}_{12}\text{O}_{22}$  hexaferrite [6, 9, 13]. No drastic changes were observed in the unit cell parameters of  $\text{Ba}_2\text{Mg}_{0.4}\text{Co}_{1.6}\text{Fe}_{12}\text{O}_{22}$  due to the similar ionic radii of  $\text{Co}^{2+}$  (0.58Å) and  $\text{Mg}^{2+}$  (0.57 Å) [14] cations.

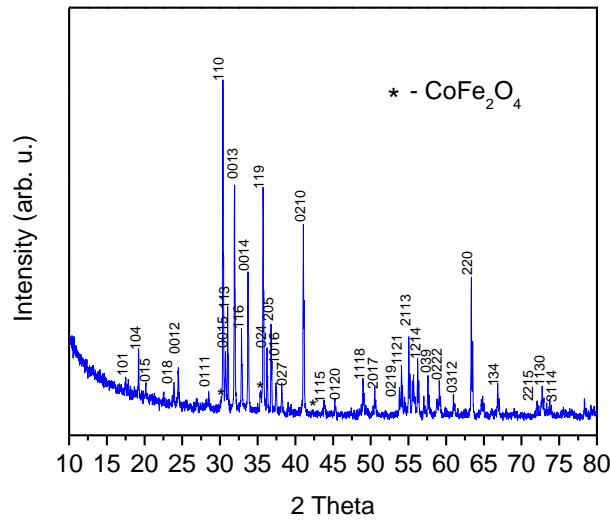


**Figure 1.** XRD pattern of the  $\text{Ba}_2\text{Mg}_{0.4}\text{Co}_{1.6}\text{Fe}_{12}\text{O}_{22}$  powder.

Iron-57 Mössbauer spectroscopy at room temperature was used to probe the oxidation state of iron ions and investigate their coordinations. Figure 2 presents the Mössbauer spectrum of  $\text{Ba}_2\text{Mg}_{0.4}\text{Co}_{1.6}\text{Fe}_{12}\text{O}_{22}$  material recorded at room temperature. The black dots and red solid lines refer to the experimental data and the fit of the spectrum, respectively. The corresponding hyperfine parameters are summarized in Table 1. The Mössbauer spectrum reveals the presence of magnetic ordering at room temperature, no doublet or singlet related to superparamagnetic particles or paramagnetic phases were observed, manifested as relatively well resolved sextets, which makes it possible to arrive at a rather unique fitting model.

The spectrum was fitted with three magnetic components corresponding to three different types of coordination of the ferromagnetic Fe atoms (tetrahedral in S and T blocks, octahedral in S and T block and octahedral in T-S block) in the structure of  $\text{Ba}_2\text{Mg}_{0.4}\text{Co}_{1.6}\text{Fe}_{12}\text{O}_{22}$  and one sextet corresponding to the  $\text{CoFe}_2\text{O}_4$  as a minor secondary phase (2%). In addition, no other impurities in the sample such as  $\text{Fe}_2\text{O}_3$  are detected, which is in good agreement with the XRD results. Indeed, a good-quality fit of the Mössbauer spectrum of  $\text{Ba}_2\text{Mg}_{0.4}\text{Co}_{1.6}\text{Fe}_{12}\text{O}_{22}$  was obtained by using four doublets attributed to three  $\text{Fe}^{3+}$  components in  $\text{Ba}_2\text{Mg}_{0.4}\text{Co}_{1.6}\text{Fe}_{12}\text{O}_{22}$  [15] and one average sextet corresponding to two  $\text{Fe}^{3+}$  sites in  $\text{CoFe}_2\text{O}_4$ . Indeed, the Mössbauer spectrum of  $\text{Ba}_2\text{Mg}_{0.4}\text{Co}_{1.6}\text{Fe}_{12}\text{O}_{22}$  is a superposition of three sub-spectra due to the three different iron positions in this material. The isomer shift values (0.27-0.38 mm/s) are typical of high spin  $\text{Fe}^{3+}$  in different environments and no ferrous form  $\text{Fe}^{2+}$  was observed. The quadrupole splitting values (-0.18-0.0 mm/s) confirm the

existence of different iron environments in the  $\text{Ba}_2\text{Mg}_{0.4}\text{Co}_{1.6}\text{Fe}_{12}\text{O}_{22}$ , that reflect three different local coordinations. The asymmetry of different iron sites is affected by the partial substitution of Co by Mg. The hyperfine magnetic fields of the three magnetic components are different 37.1, 40.7 and 43.1 T, which agreed with the previous studies [15]. The occupancy of Fe ions at the three crystallographic positions in the structure can be obtained from the relative area of each sextet in the corresponding Mössbauer spectrum by assuming similar Mössbauer Lamb factors for all sites. The three sub-spectral components show different relative intensities of 50%, 21%, and 27% good agreement with the reported results in the literature.

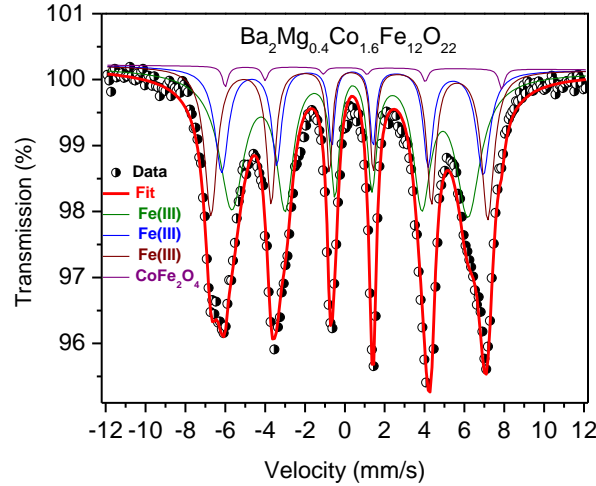


**Figure 2.** The Mössbauer spectrum recorded at room temperature of  $\text{Ba}_2\text{Mg}_{0.4}\text{Co}_{1.6}\text{Fe}_{12}\text{O}_{22}$  material.

**Table 1.** Hyperfine parameters<sup>1</sup> of the room-temperature Mössbauer spectrum of  $\text{Ba}_2\text{Mg}_{0.4}\text{Co}_{1.6}\text{Fe}_{12}\text{O}_{22}$ .

Iron sites	$\delta$ (mm s <sup>-1</sup> )	$\Delta$ (mm s <sup>-1</sup> )	$\Gamma$ (mm s <sup>-1</sup> )	$B_{\text{hf}}$ (T)	Area (%)
a-Fe(III)	0.34 (1)	-0.18 (1)	0.40 (1)	37.1 (1)	50 (1)
b-Fe(III)	0.38 (2)	0.00	0.28 (2)	40.7 (1)	21 (1)
c-Fe(III)	0.27 (1)	-0.09 (1)	0.28 (1)	43.1 (1)	27 (1)
$\text{CoFe}_2\text{O}_4$	0.48 (2)	0.92 (2)	0.33 (1)	43.0 (1)	2 (1)

<sup>1</sup>  $\delta$  – Isomer shift, referred to  $\alpha$ -iron at 295 K;  $\Delta$  – quadrupole splitting,  $\Gamma$  – linewidth,  $B_{\text{hf}}$  – hyperfine field.

The hysteresis loops of the powder material at room temperature and 4.2 K are displayed in Figure 3 and provide evidence that the amount of cobalt ferrite was unable to affect appreciably the basic magnetic properties of the material. The magnetic parameters, namely, the magnetization at 50 kOe, the remanent magnetization ( $M_r$ ) and the coercivity field ( $H_c$ ) obtained from the curves are listed in Table 2.

**Table 2.** Magnetic properties of  $\text{Ba}_2\text{Mg}_{0.4}\text{Co}_{1.6}\text{Fe}_{12}\text{O}_{22}$ .

Sample	T K	M (50 kOe) emu/g	$M_r$ emu/g	$H_c$ Oe
$\text{Ba}_2\text{Mg}_{0.4}\text{Co}_{1.6}\text{Fe}_{12}\text{O}_{22}$	300	26.6	low	2
$\text{Ba}_2\text{Mg}_{0.4}\text{Co}_{1.6}\text{Fe}_{12}\text{O}_{22}$	4.2	30.0	low	48

The coercivity field was determined from the hysteresis curve as the half of the difference of the magnetic field value at zero magnetization. The magnetization values  $M$  measured at a magnetic field of 50 kOe were 30 emu/g and 26.6 emu/g at 4.2 K and 300 K, respectively. These values lie between the values reported for non-substituted  $\text{Ba}_2\text{Mg}_2\text{Fe}_{12}\text{O}_{22}$  and  $\text{Ba}_2\text{Co}_2\text{Fe}_{12}\text{O}_{22}$  [5], but they do not differ significantly from those for  $\text{Ba}_2\text{Mg}_2\text{Fe}_{12}\text{O}_{22}$  powder material prepared under similar condition [11]. The hysteresis curve at 300 K is very narrow (about 4 Oe), while  $H_c$  is about 2 Oe. This value is typical

for the hexaferrites with planar magneto-crystalline anisotropy. The inset in Figure 3a shows a triple hysteresis loop at 4.2 K in the low magnetic field range that indicates the presence of two kinds of ferromagnetic states with different magnetization values. The  $M_r$  values are very low, which yields also a very low squareness ratio ( $M_r/M_s$ ), indicating a multi-domain structure of the particles in the powder.

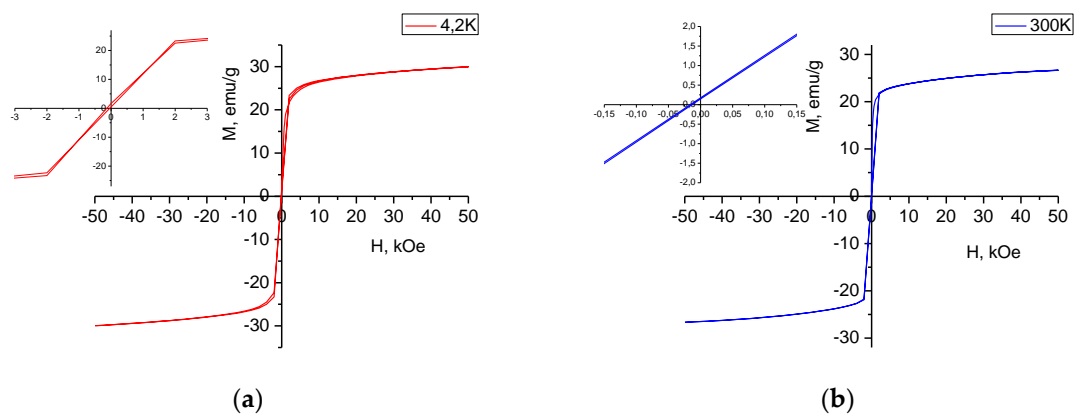


**Figure 3.** Hysteresis curves (a) at 4.2 K and (b) 300 K. The insets in (a) and (b) show the magnetization around zero magnetic field.

The magnetic-phase transition temperature can be determined from the temperature dependence of the magnetization at a fixed applied magnetic field. The temperature dependence of the ZFC and FC magnetization curves of the  $\text{Ba}_2\text{Mg}_{0.4}\text{Co}_{1.6}\text{Fe}_{12}\text{O}_{22}$  powder material at magnetic fields of 50 Oe, 100 Oe and 500 Oe in the temperature range 4.2 – 300 K are presented in Figure 4.

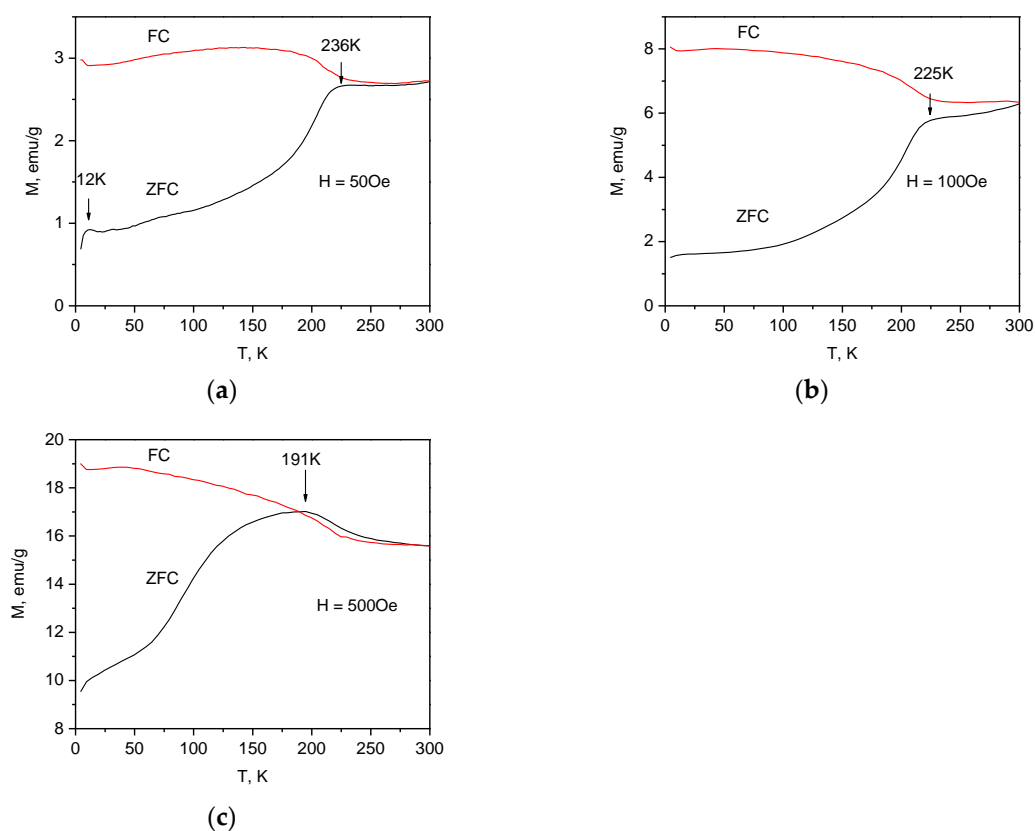


**Figure 4.** Temperature dependence of ZFC- and FC-magnetization at a magnetic field of (a) 50 Oe, (b) 100 Oe and (c) 500 Oe.

As it can be seen in the Figure 4a, with increasing the temperature above 4 K the ZFC magnetization rises very rapidly up to 12 K. This finding was clearly pronounced only in a field of 50 Oe (see Figure 4a) and becomes smeared at higher magnetic fields (see Fig. 4b). Then it rises slowly up to 115 K followed by a more rapid increase between 116 K and 225 K. The magnetization reaches its maximum at 236 K and remains practically constant with the further rise of the temperature. At low temperatures, the ZFC magnetization at a field of 100 Oe slowly increases with rising temperature and then rises rapidly between 120 K and 215 K; this is followed by a slow increase (Figure 4b). The first derivative of the ZFC magnetization vs. temperature curve shows a maximum at 204 K, which corresponds to an inflection point of the  $M_{ZFC}$  vs.  $T$  curve, a fact indicating the onset of a magnetic phase transition ending at 225 K. In the 204 – 225 K interval, the so-called intermediate phase exists, which is a mixture of collinear and helical spin orders. The ZFC magnetization vs. temperature for a field of 500 Oe has a somewhat different behavior than those for fields of 50 Oe and 100 Oe. It rises rapidly up to 180 K, reaches its maximum at 191 K and then decreases. As seen in Figure 4c, a superposition of the ZFC and FC curves takes place at 285 K.

The maximum observed in the ZFC-magnetization curves is related to a magnetic phase transition from a ferrimagnetic to a helical spin order. This transition determines the multiferroic properties of this material. A similar behavior was reported for  $Ba_2Co_{2-x}Zn_xFe_{12}O_{22}$  [16]. The temperature of this magnetic phase transition decreased as the magnetic field was increased and is higher than that of undoped sample. No anomalies were seen in the ZFC- and FC-magnetization curves around 40 K, while such behaviors were observed for a non-substituted  $Ba_2Mg_2Fe_{12}O_{22}$  sample [13].

#### 4. Conclusions

$Ba_2Mg_{0.4}Co_{1.6}Fe_{12}O_{22}$  powder material was prepared by the sonochemical co-precipitation route. The substantial cobalt substitution for magnesium in the  $Ba_2Mg_2Fe_{12}O_{22}$  basic composition did not lead to a significant change of the unit cell parameters. However, the ZFC-FC magnetization curves were recorded under different magnetic fields revealed that the magnetic phase transition from a ferrimagnetic to a helical spin order known to occur in single crystals is shifted to the temperature range 191-236 K depending on the applied magnetic field. Thus, the  $Co^{2+}$  substitution in the Y-type  $Ba_2Mg_2Fe_{12}O_{22}$  hexaferrite leads to an increase of the magnetic phase transition temperature to the specific helical spin arrangement believed to be a precondition for the multiferroic properties of the undoped material.

**Author Contributions:** T.K. and S.K. conceptualization; T.K., S.K., K.K. conceived and designed the experiments; T.K. and B.G. materials synthesis; D.K., R.C. and B.V. did XRD analysis and refinements; A.M. and F.B. did Mössbauer measurements and analysis; L.M.T. and A.Z. did magnetic measurements; L.M.T., A.Z., T.K., S.K., K.K. and B.G. contributed the magnetic measurements analysis; T.K., S.K., D.K., B.V., A.M., K.K. discussed the results; T.K., S.K., A.M., Ch.Gh. and K.K. wrote the manuscript; Ch.Gh. reviewed & edited the final version

**Acknowledgments:** The work was supported by the Bulgarian National Science Fund under contract DN 08/4 “Novel functional ferrites-based magneto-electric structures”, by a joint research project between the Bulgarian Academy of Sciences and WBI, Belgium, and by a joint research project between the Bulgarian Academy of Sciences and the Institute of Low Temperature and Structure Research, Polish Academy of Sciences. . A. Mahmoud is grateful to the Walloon region for a Beware Fellowship Academia 2015-1, RESIBAT n° 1510399.

**Conflicts of Interest:** The authors declare no conflict of interest.

#### References

1. Cheong, S.-W.; Mostovoy, M. Multiferroics: a magnetic twist for ferroelectricity. *Nat. Mater.* **2007**, *6*, 13-20, DOI 10.1038/nmat1804
2. Kida, N.; Kumakura, S.; Ishiwata, S.; Taguchi, Y.; Tokura, Y. Gigantic terahertz magnetochromism via electromagnons in the hexaferrite magnet  $Ba_2Mg_2Fe_{12}O_{22}$ . *Phys. Rev. B* **2011**, *83*, art. num. 064422, DOI 10.1103/PhysRevB.83.064422.
3. Kimura, T. Magnetolectric Hexaferrites. *Annu. Rev. Condens. Matter Phys.* **2012**, *3*, 93-100, DOI 10.1146/annurev-conmatphys-020911-125101

4. Taniguchi, K.; Abe, N.; Ohtani, S.; Umetsu, H.; Arima, T. Ferroelectric polarization reversal by a magnetic field in multiferroic Y-type hexaferrite  $\text{Ba}_2\text{Mg}_2\text{Fe}_{12}\text{O}_{22}$ . *Appl. Phys. Express* **2008**, *1*, 031301, DOI 10.1143/APEX.1.031301
5. Pullar, R.C. Hexagonal ferrites: A review of the synthesis, properties and applications of hexaferrite ceramics. *Prog. Mater. Sci.* **2012**, *57*, 1191-1334, DOI 10.1016/j.pmatsci.2012.04.001
6. Momozava, N.; Yamaguchi, Y.; Mita, M. Magnetic structure change in  $\text{Ba}_2\text{Mg}_2\text{Fe}_{12}\text{O}_{22}$ . *J. Phys. Soc. Jpn.*, **1986**, *55*, 1350-1358, DOI 10.1143/JPSJ.55.1350.
7. Nakamura, S.; Tsunoda, Y.; Fuwa, A. Moesbauer Study on Y-type hexaferrite  $\text{Ba}_2\text{Mg}_2\text{Fe}_{12}\text{O}_{22}$ . *Hyperfine Interact.*, **2012**, *208*, 49-52, DOI 10.1007/s10751-011-0486-2
8. Tokura, Y.; Seki, Sh. Multiferroics with spiral spin orders. *Adv. Mater.*, **2010**, *22*, 1554-1565, DOI 10.1002/adma.200901961
9. Ishiwata, Sh.; Okuyama, D.; Kakurai, K.; Nishi, M.; Taguchi, Y.; Tokura, Y. Neutron diffraction studies on the multiferroic conical magnet  $\text{Ba}_2\text{Mg}_2\text{Fe}_{12}\text{O}_{22}$ . *Phys. Rev. B*, **2010**, *81*, 174418, DOI 10.1103/PhysRevB.81.174418
10. Georgieva, B.; Krezhov, K.; Kolev, S.; Ghelev, Ch.; Kovacheva, D.; Fabian, M.; Svab, E.; Koutzarova, T. Characterization of Y-type hexaferrite  $\text{Ba}_2\text{Mg}_2\text{Fe}_{12}\text{O}_{22}$  powders. IEEE Proc. 40<sup>th</sup> International Spring Seminar on Electronics Technology, Sofia, Bulgaria, 10-14 May 2017, (2017) pp. 39-44; IEEE, DOI 10.1109/ISSE.2017.8000885
11. Koutzarova, T.; Kolev, S.; Nedkov, I.; Krezhov, K.; Kovacheva, D.; Ghelev, C.; Vertruyen, B.; Henrist, C.; Cloots, R. Study of quasi-monophase Y-type hexaferrite  $\text{Ba}_2\text{Mg}_2\text{Fe}_{12}\text{O}_{22}$  powder. *Micro and Nanosystems* **2014**, *6*, 14-20, DOI 10.2174/187640290601140919123530
12. Jotania, R.B.; Virk, H.S. Y-Type Hexaferrites: Structural, Dielectric and Magnetic Properties. *Solid State Phenomena* **2012**, *189*, 209-232, DOI 10.4028/www.scientific.net/SSP.189.209
13. Koutzarova, T.; Kolev, S.; Nedkov, I.; Krezhov, K.; Kovacheva, D.; Blagoev, B.; Ghelev, C.; Henrist, C.; Cloots, R.; Zaleski, A. Magnetic properties of nanosized  $\text{Ba}_2\text{Mg}_2\text{Fe}_{12}\text{O}_{22}$  powders obtained by auto-combustion. *J. Supercond. Novel Magnetism* **2012**, *25*, 2631-2635, DOI 10.1007/s10948-011-1232-3
14. Database of Ionic Radii, Atomistic Simulation Group in the Materials Department of Imperial College <http://abulafia.mt.ic.ac.uk/shannon/ptable.php>
15. Mahmood, S.H.; Jaradat, F.S.; Lehlooh; Hammoudeh, A. Structural properties and hyperfine interactions in Co-Zn Y-type hexaferrites prepared by sol-gel method. *Ceram. Int.* **2014**, *40*, 5231-5236, DOI 10.1016/j.ceramint.2013.10.092
16. Lim J.T.; Kim C.S. Magnetic properties of Zn doped  $\text{Co}_2\text{Y}$  hexaferrite by using high-field Mössbauer spectroscopy. *J. Appl. Phys.* **2014**, *115*, 17A516, DOI 10.1063/1.4865879

